

## Vortex rectification effects in films with periodic asymmetric pinning

J. Van de Vondel,<sup>1</sup> C. C. de Souza Silva,<sup>1</sup> B. Y. Zhu,<sup>2</sup> M. Morelle,<sup>1</sup> and V. V. Moshchalkov<sup>1,\*</sup>

<sup>1</sup>Nanoscale Superconductivity and Magnetism Group,  
Laboratory for Solid State Physics and Magnetism,  
K. U. Leuven, Celestijnenlaan 200 D, B-3001 Leuven, Belgium  
<sup>2</sup>Quantum Phenomena Observation Technology Laboratory,  
The Institute of Physical and Chemical Research (RIKEN) and Advanced  
Research Laboratory Hitachi Ltd. Hatoyama, Saitama 350-0395, Japan

We study the transport of vortices excited by an ac current in an Al film with an array of nanoengineered asymmetric antidots. The vortex response to the ac current is investigated by detailed measurements of the voltage output as a function of ac current amplitude, magnetic field and temperature. The measurements revealed pronounced voltage rectification effects which are mainly characterized by the two critical depinning forces of the asymmetric potential. The shape of the net dc voltage as a function of the excitation amplitude indicates that our vortex ratchet behaves in a way very different from standard overdamped models. Rather, as demonstrated by the observed output signal, the repinning force, necessary to stop vortex motion, is considerably smaller than the depinning force, resembling the behavior of the so-called inertia ratchets. Calculations based on an underdamped ratchet model provide a very good fit to the experimental data.

PACS numbers: 05.40.-a, 74.78.Na., 74.40.+k, 85.25.-j

From the point of view of classical thermodynamics, it is not possible to induce directed motion of particles by using equilibrium fluctuations only, otherwise it would constitute a perpetual mobile of the second kind [1]. Nevertheless, non-equilibrium fluctuations, such as periodic excitations or a "colored" noise, are allowed to take advantage of the asymmetry of a periodic ratchet potential to promote motion of particles in a preferential direction [2]. New solid-state-based ratchet systems are currently being developed for controlling the motion of electrons [3] and fluxons, as well as for particle separation [4] and electrophoresis [5]. In particular, ratchet potentials in superconducting devices may be very useful to control the dissipative motion of fluxons, which causes undesired internal noise.

Modern lithographic techniques make it possible to fabricate periodic arrays of vortex pinning sites with size and shape that can be easily tuned, thus giving an interesting perspective for making different asymmetric pinning potentials. In this context, several ideas to control flux motion by applying an ac excitation have been proposed [6, 7, 8, 9], but up to now only a few experiments have been realized [10, 11]. One realization has been recently implemented on a Nb film with a square array of nanoscopic triangular magnetic dots [10]. The authors reported rectification of the ac driven vortices due to the asymmetric shape of the dots. Nevertheless, the detailed dynamics of vortices in such structures is not yet completely understood.

In this Letter we investigate a composite square array of pinning sites, with its unit cell consisting of a small and a big square antidot separated by a narrow superconducting wall, as a vortex rectifier. As demonstrated by our dc and ac transport measurements at several fields and temperatures, this configuration is able to break the

reflection symmetry of the total effective pinning potential and promote flux quanta rectification. Moreover, our data reveals a remarkable hysteresis in the current-induced pinning-depinning process. This gives an apparent inertia to the system with important consequences in the overall dynamics. Finally, we discuss how standard overdamped models fail in describing these results and propose an underdamped ratchet model that provides a very good fit to our experimental data.

The pattern was prepared by electron-beam lithography on a SiO<sub>2</sub> substrate. The superconducting thin film is a 38 nm thick Al, in a 5 × 5 mm<sup>2</sup> cross-shaped geometry [see Fig. 1.(a)] to allow four-point electrical transport measurements in two perpendicular current directions. The central part of the cross consists of two 300-μm-wide strips containing the nanoengineered array (period  $a_p = 1.5 \mu\text{m}$ ) of asymmetric pinning sites [see Fig. 1.(b)]. This gives a value of 0.92 mT for the first matching field,  $H_1 = \phi_0/a_p^2$  (here  $\phi_0 = h/2e$  is the flux quantum). In each strip, the voltage contacts are 2 mm apart. The

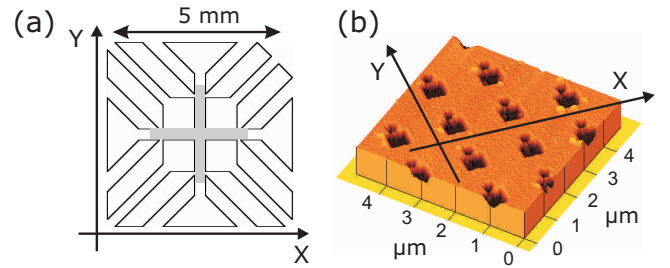


FIG. 1: Layout of the Al film. (a) Cross-shaped geometry of the sample to allow for transport measurements in the x and y directions. (b) atomic force micrograph of a 5 × 5 μm<sup>2</sup> area of the asymmetric pinning sites

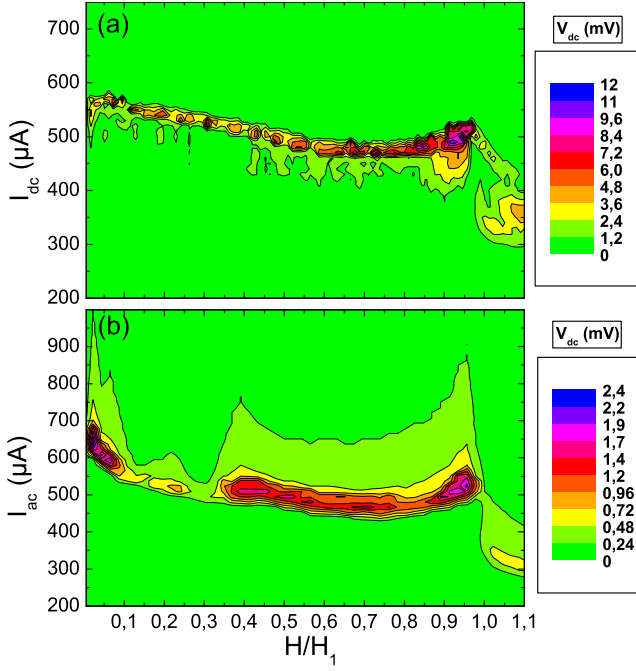


FIG. 2: (a) Contour plot of the magnetic field and dc current dependence of the voltage difference for dc currents applied in the  $x$  and  $-x$  direction  $V(I_x; H) - V(I_x; H)$  at  $T = T_c = 0.973$  (b) Contour plot of the net dc voltage  $V_{dc}(I_{ac}; H = H_1)$  as a function of the magnetic field and amplitude of the ac sinusoidal current at a frequency 1 kHz and  $T = T_c = 0.973$ .

sizes of the small and big antidots are  $300 \times 300 \text{ nm}^2$  and  $600 \times 600 \text{ nm}^2$  with a separation between them of 90 nm. The magnetic field was applied perpendicularly to the sample surface. The superconducting critical temperature ( $T_c = 1.469 \text{ K}$ ,  $4 \text{ T} = 3 \text{ mK}$ ) was obtained by using a resistance criterion of 10% of the normal state resistance. From the residual resistivity at 4.2 K, the elastic mean free path ( $l_{e1} = 3.9 \text{ nm}$ ) was found. From this we can calculate the coherence length ( $\xi(0) = 67.5 \text{ nm}$ ) and the penetration length ( $\lambda(0) = 195 \text{ nm}$ ) using the dirty limit expressions. We can therefore conclude that the patterned film with the composite array of square antidots is a type-II superconductor ( $\kappa = \frac{\lambda(0)}{\xi(0)} = 2.89 > \kappa_{1/2}^1 = 0.71$ ).

Fig. 2 (a) shows a contour plot of the magnetic field and current dependence of the difference in induced voltage for the dc currents flowing in the positive and negative  $x$  direction,  $V(I_x; H) - V(I_x; H)$ , at 97.3 % of the critical temperature. The voltage drop in the  $x$  direction is a measure of the vortex velocity in the  $y$  direction. Since the  $I_x$  and  $I_x$  dc currents induce a Lorentz force in the negative and positive  $y$  directions, the vortices will probe the asymmetry of the pinning sites. We see that for all fields ( $0 < H/H_1$ ) there is a dc voltage difference confirming the presence of an asymmetry in the pinning potential. This difference is the largest for fields just below the first matching field,  $H_1$ , which can be explained

by the high symmetry of the vortex configuration which cancels out the vortex-vortex interactions. In this case the resulting forces acting on vortices are coming only from the asymmetric pinning potential. To get the data shown in Fig. 2 (b), a 1 kHz sinusoidal current was applied to the sample and the output signal was measured with an oscilloscope used as an analog-digital converter. Integrating this signal gives the average dc response, which is plotted as a function of the normalized magnetic field,  $H = H_1$ , and amplitude of the applied current,  $I_{ac}$ . A gain, we can clearly see a ratchet effect at all fields from 0 to  $1.1H_1$ . This effect is maximum just below  $H_1$  and  $\frac{1}{2}H_1$ , where vortex-vortex interactions are also mostly cancelled. The measurements carried out at other temperatures ( $T = T_c = 0.967$  up to  $T = T_c = 0.98$ ) show similar features. Nevertheless, the rectification effect is weaker at higher temperatures, which can be explained by an increase in  $\lambda(T)$  and  $\xi(T)$ , making the size of the vortices big compared to the antidot size. In this case the vortices cannot sense the asymmetry anymore. We have also repeated the measurements for several frequencies in the range 10 Hz to 10 kHz. No significant change in the results was observed, which means that our experiments are carried out deep in the adiabatic regime [2].

As it is clearly seen from the vertical scans in Fig. 2 (b), the net dc voltage increases sharply with the ac-current amplitude up to a maximum value and then decays smoothly to zero. This is a typical behavior of ac-driven objects in a ratchet potential in the adiabatic regime. At low frequencies, the net dc flow hvi of particles increases monotonically when the excitation amplitude  $A$  is between the weaker,  $f_{d1}$ , and the stronger,  $f_{d2}$ , depinning forces of the asymmetric potential. We shall refer to this region as the rectification window. Since in this amplitude range the force cannot overcome the potential barrier for negative force direction, motion occurs only during the positive half loops of the ac excitation, that is, the system behaves as a half-wave rectifier. For amplitudes  $A > f_{d2}$ , the particles are allowed to travel back and forth, thus leading to a decrease in the rectification signal, which vanishes slowly at high drives as the ratchet potential is gradually averaged out by the fast-moving particles. It is worth noting that these general properties of the ratchet effect also depend on the shape of the ac excitation [2]. For instance, square-wave excitations lead to sharper rectification effect and a shorter tail in the hvi- $A$  characteristics as compared to sinusoidal excitations. Since the regime of the dc measurements is equivalent to irradiating the system with a square wave pulse, the dc data presented in Fig. 2 (a) looks much sharper than the ac data shown in Fig. 2 (b).

A closer look at the ac-amplitude dependence of the net dc voltage reveals additional and important features of the ratchet dynamics in our system. Figs. 3 and 4 show detailed dc voltage versus ac amplitude ( $V_{dc}-I_{ac}$ ) characteristics. For fields below the first matching field some

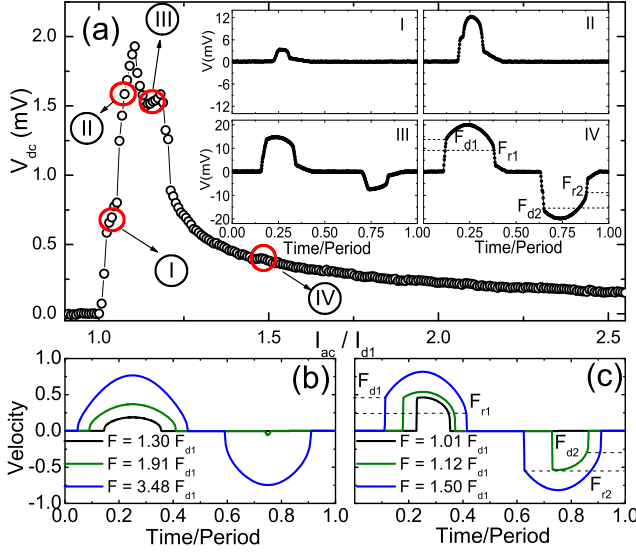


FIG. 3: Net dc voltage as a function of ac amplitude at  $H = H_1 = 0.96$  and  $T = T_c = 0.973$ . The current is normalized by the  $I_{d1} = 473$  A. Inset: Voltage output at the ac amplitudes (I) 477 A, (II) 502 A, (III) 544 A and (IV) 704 A; (a) time evolution of the vortex velocity  $v(t)$  from an overdamped molecular dynamics simulation (see text); and (b)  $v(t)$  calculated from the inertia ratchet model. The horizontal dashed lines indicate the instantaneous value of excitation where vortices are depinned [ $F(t) = F_d$ ] and repinned [ $F(t) = F_r$ ]. The subscripts 1 and 2 stand for the weaker and the stronger depinning forces respectively.

$V_{dc}$ - $I_{ac}$  curves, as the one at  $H = 0.96H_{c1}$  (Fig. 3), have two peaks. Detailed measurements of the time evolution of the output voltage  $V(t)$ , indicated by roman numbers, suggest a superposition of two ratchet effects. Rectification is first triggered just above  $I_{ac} = 473$  A and the output signal is present only at the positive half-loop of the ac current, as shown in panel I. At  $I_{ac} = 495$  A, a stronger ratchet is triggered. It can be identified in panel II as a second jump in the signal in the positive half-loop. Right above  $I_{ac} = 520$  A a small signal in the negative half loop appears (see panel III), thus demonstrating that the weaker ratchet is already outside its rectification window. In panel IV, the signal is strong in both directions, indicating that the driven vortex lattice moves back and forth as a whole. A possible reason for the presence of two ratchets can be a complicated plastic dynamics in which vortex channels flow along specific rows of pinning centers for currents considerably lower than the depinning current of the whole vortex lattice. Plastic dynamics was thoroughly studied by numerical simulations in periodic arrays of symmetrical pinning centers [12]. The local decrease in pinning efficiency in a given pinning row is caused by discommensurations (vacant pinning sites for fields  $H < H_1$ ) distributed along the row. The extension of these ideas to arrays of asymmetric pinning sites seems to be rather straightforward. At fields very close or at  $H_1$

this effect is minimized. At  $H = 0.98H_1$  for instance, the  $V_{dc}$ - $I_{ac}$  characteristic, shown in Fig. 4, presents a single well-defined rectification peak.

Another remarkable feature disclosed in the  $V(t)$  data is that the repinning force  $f_r$  necessary to stop vortex motion in either direction is always smaller than the corresponding depinning force  $f_d$  [see Fig. 3, insets (I)-(IV)]. In other words, the  $V$ - $I$  characteristic is hysteretic. This is a very robust phenomenon which has been observed in the whole field, frequency and temperature ranges used in our experiment and, to the best of our knowledge, has not been reported before. To understand the experimental results, we have performed molecular dynamics (MD) simulations of the overdamped equations of motion for vortices in a square array of asymmetric pinning potentials at fields close to the  $H_1$  and subjected to a sinusoidal Lorentz force of very low frequency (the details of the model and simulations are reported in Ref. [9]). In the whole range of excitation amplitudes, no hysteresis was observed ( $f_r = f_d$ ), the  $v(t)$  curves at each half period are symmetrical, in contrast with the clearly asymmetrical shape of the  $V(t)$  experimental data. In addition, the hvi- $A$  characteristics look qualitatively different from the experimental results. A possible reason for the mismatch between the MD calculations and the experimental results is that the depinning process of an overdamped particle is reversible because it carries no significant inertia and cannot be deformed. However, vortices are soft objects that can be deformed under the action of competing forces and they also carry a small mass. In the dirty limit, the vortex mass can be several times smaller than the electron mass. In this case, inertia is only relevant at frequencies typically above  $10^{12}$  Hz [13]. Since our sample is in the dirty limit, we believe the contribution of vortex mass is negligible in our experiment. Therefore, the apparent inertia is more likely due to vortex deformation. Indeed, recent numerical simulations of the Ginzburg-Landau equations [14] suggested that the current-induced depinning of vortices in a periodic array of antidots is dominated by strong elongation of the vortex cores towards a neighboring antidot. Interestingly, the authors observed hysteresis in the pinning-depinning process resulting from this behavior.

To illustrate how this hysteresis influences the overall ratchet dynamics, we model vortices still as rigid particles but carrying an apparent mass  $M$ . For simplicity, we consider that the vortex lattice is perfectly commensurate with the pinning array and therefore we shall analyze the experimental results measured very close to the first matching field ( $H = 0.978H_1$ ) shown in Fig. 4. In this case, due to the cancellation of the vortex-vortex interactions, the vortex dynamics can be reduced to that of one particle moving in a one-dimensional potential. The corresponding equation of motion is

$$M \frac{dv}{dt} = -v \left( \frac{\partial}{\partial x} \right) (U(x) + A \sin(\omega t)); \quad (1)$$

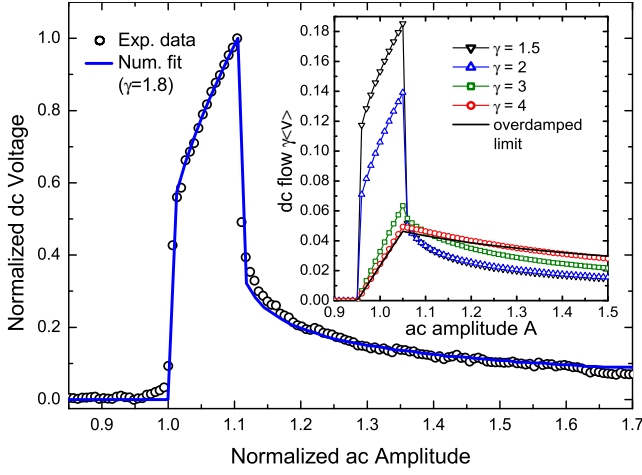


FIG. 4: Normalized dc voltage as a function of ac amplitude. Circles: experimental data at  $H = H_1 = 0.98$  and  $T = T_c = 0.973$ . Line: numerical fit using the inertia ratchet model [Eq. (1)] with only one fitting parameter,  $\gamma = 1.8$ . Inset: numerical integration of the inertia ratchet model for different  $\gamma$  (symbols) and the overdamped limit solution (line).

where  $\eta$  is the viscous drag coefficient,  $v$  is the instantaneous vortex velocity and  $U_p(x)$  is the one-dimensional pinning potential, which we choose in a simple form as  $U_p(x) = U [\sin(2x/a_p) + 0.025 \sin(4x/a_p)]$ . This gives an asymmetry ratio  $f_{d1} = f_{d2} = 0.925$  similar to that observed in our data shown in Fig. 4 ( $I_{d1} = 480$  A and  $I_{d2} = 519$  A). In order to be closer to the experimental conditions, we will restrict ourselves to the adiabatic regime, that is, we shall consider only frequencies much lower than the libration frequency of the pinning potential!  $\omega_p \ll \omega$  and the viscous drag to mass ratio  $\eta/m \ll \omega$ .

In this way, by normalizing the ac amplitude by the first depinning force and the dc response by maximum response, the only fitting parameter for comparing the calculations with the experimental data is  $\gamma$ .

The overdamped limit corresponds to  $\eta/m \rightarrow 0$ , or, equivalently, to  $\gamma \rightarrow 0$ . In this limit a semi-analytical approach may be used. The average flow of vortices in one cycle of the ac excitation is given by  $\langle v \rangle = \frac{1}{P} \int_0^P dt v(t)$  where  $P = 2\pi/\omega$  is the forcing period and

$$v(t) = -\frac{R_{ap}}{U_p(x) + A \sin(\omega t)} : \quad (2)$$

This model reproduces exactly the MD simulations for  $H = H_1$ . The hvi-A characteristic calculated for the overdamped limit is given by the full line in the inset of Fig. 4. The curve presents a long and slowly decaying tail qualitatively different from the curves observed in our experiments.

For finite values, we integrate Eq. 1 numerically by a finite difference method. The results for several values (in units of  $\eta/m = 2$ ) are shown in the inset of Fig. 4. For

$\gamma = 4$ , the hvi-A characteristic is already very close to the overdamped limit. For smaller values, the effect of inertia becomes increasingly more pronounced. The curves look sharper and more restricted to the rectification window. As shown in the main frame of this figure, the  $\gamma = 1.8$  curve provides an excellent fitting to the experimental data. The time evolution of the velocity  $v(t)$  for  $\gamma = 1.8$  is shown in the inset (b) of Fig. 3 for a few ac drive values. Note that the curves correctly reproduce the asymmetry observed in the experimental  $V(t)$  data [insets (I)-(IV)], with  $F_r \neq F_d$ . The  $v(t)$  curves calculated for  $\gamma = 4$  resemble the overdamped limit [Eq. 2], which gives exactly  $F_d = F_r$  and no hysteresis.

In conclusion, we have demonstrated voltage rectification in a superconducting film with a composite periodic array of asymmetric pinning sites. The rectification was observed in dc and ac measurements in a broad field range and for different temperatures, showing that our sample provides a two-dimensional asymmetric potential which is able to control vortex motion. For fields below the first matching field, our data revealed a competition between two ratchet dynamics, which can be understood as the competition between plastic channelling dynamics and coherent vortex motion. We also have observed a strong irreversibility in the pinning-depinning process, which we believe is due to current-induced elongation of the vortex core. Calculations based on an underdamped ratchet model provided a very good fit to the experimental data and showed that the hysteresis found in our experiment gives rise to an apparent inertia with important consequences to the ratchet dynamics.

This work was supported by the K.U. Leuven Research Fund GOA/2004/02 and FWO programs. C.C.S.S. acknowledges the support of the Brazilian Agency CNPq. M.M. acknowledges support from the Institute for the Promotion of Innovation through Science and Technology in Flanders (IW-T-Vlaanderen).

Electronic address:

Victor Moshchalkov@fyskuleuven.ac.be

- [1] M. von Smoluchowski, Phys. Z. X III, 1069 (1912); R. P. Feynman et al., The Feynman Lectures on Physics (Addison-Wesley, Reading, MA, 1963).
- [2] For a review see P. Reimann, Phys. Rep. 361, 57 (2002).
- [3] H. Linke et al., Appl. Phys. A 75, 237 (2002).
- [4] S. M. Athias and F. Müller, Nature 424, 53 (1999).
- [5] C. Marquet et al., Phys. Rev. Lett. 88, 168301 (2002).
- [6] C.-S. Lee et al., Nature 400, 337 (1999).
- [7] J. F. Wambaugh et al., Phys. Rev. Lett. 83, 5106 (1999).
- [8] C. J. Olson et al., Phys. Rev. Lett. 87, 177002 (2001).
- [9] B. Y. Zhu et al., Phys. Rev. B 68, 014514 (2003); Phys. Rev. Lett. 92, 180602 (2004).
- [10] J. E. Villegas et al., Science 302, 1188 (2003).
- [11] R. W.ördenweber et al., Phys. Rev. B 69, 184504 (2004).
- [12] C. Reichhardt et al., Phys. Rev. B 58, 6534 (1998).

[13] H. Suhl, Phys. Rev. Lett. 14, 226 (1965).

[14] D. J. Priour and H. A. Fertig, Phys. Rev. B 67, 054504

(2003).